Supplementary Information for

Paired Electrosynthesis Enabled by Hydrogen Atom Redox-Relay Strategy

Siyun Dai, [a,c] Yang Li, [a,c] Wei Qu,[c] Jun Xuan,[c] Xili Cui,[a,b,c] Yiming Mo*[a,c], and Huabin Xing [a,b,c]

[a] *College of Chemical and Biological Engineering, Zhejiang University, Hangzhou, 310027, Zhejiang, China*

[b] *Engineering Research Center of Functional Materials Intelligent Manufacturing of Zhejiang Province, ZJU-Hangzhou Global Scientific and Technological Innovation Center, Hangzhou, 311215, China*

[c] *Key Laboratory of Biomass Chemical Engineering of Ministry of Education, College of Chemical and Biological Engineering, Zhejiang University, Hangzhou, 310027, China*

*Corresponding Author

E-mail: yimingmo@zju.edu.cn

Table of contents

1 Supplementary figures and tables

Table S1. Comparison of the hydrogen and electron storage densities of LaNi$_5$ alloy with other materials.

	LaNi$_5$ alloy	Methylcy-clohexane[1]	18H-dibenz-yltoluene[1]	Ammonia[1]
Hydrogen density by volume (kg/m^3)	117.6	47.3	56.4	121
	AB$_5$-2 RR-electrode	**NaNiHCF-10 electrode[2]**	**NiHCF electrode[3]**	**Ni(OH)$_2$ electrode[4]**
Electron capacity by weight (mmol/g)	7.9	2.5	2.4	8.4
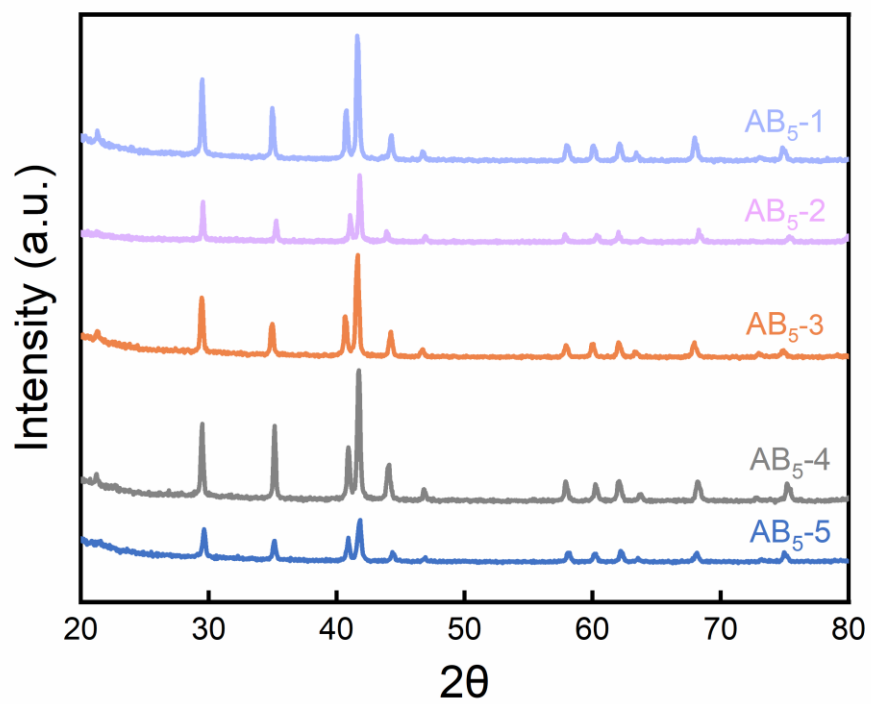
Fig.S1. Comparison of the XRD patterns collected on various AB$_5$-type alloys.
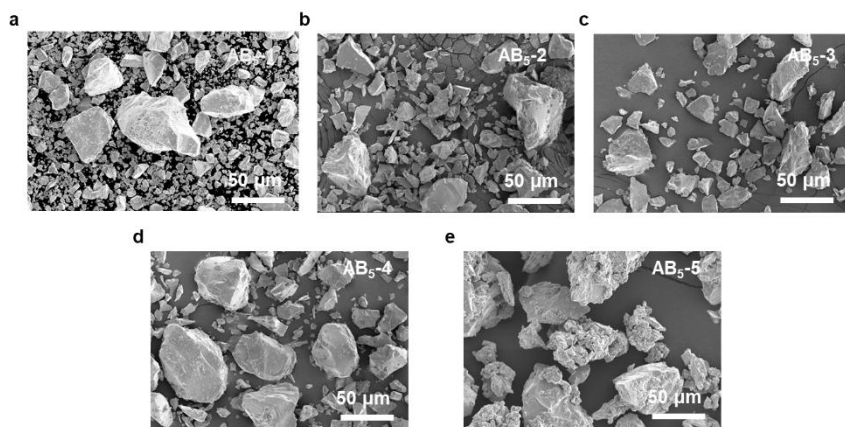
Fig.S2. The SEM images of the five AB₅-type alloys (a, b, c, d, e). AB₅-1 alloy, obtained from Alfa Aesar, has a wide range of particle sizes and requires sieving before use. AB₅-2 to AB₅-4 alloys (b-d) were pre-sieved to obtain particles with diameters ranging from 20 to 100 μm. AB₅-5 alloy (e) was obtained from battery, which had undergone a forming process, resulting in the observation of adhesive residues in the image.

Note S1. Selection of electrode binders.

Among several widely utilized binders[5–9], Nafion is relatively expensive. Poly(vinylidenedifluoride) (PVDF) exhibits a significant swelling in various electrolytes, and degrades severely in alkaline solutions by dehydroflurination[6,7]. Carboxymethyl cellulose (CMC) has a poor mechanical property[8]. Polytetrafluoroethylene (PTFE) appears as a suitable binder for RR-electrode for its excellent chemical and electrochemical stability as well as a good adhesive property. The PTFE-contained (10 wt%) electrodes have been reported to exhibit a superior cycle stability compared to the PVDF- and Nafion-binded electrodes[6]. Excessive binder additives may have a cladding effect on the alloy[5,10] can decrease the active surface area of the alloy material, resulting in a reduced hydrogen storage capacity and increased ohmic resistivity. The final weight percentages of the binder and conductive carbon material were both set to 5 wt% to ensure good adhesion strength and conductivity[11,12].
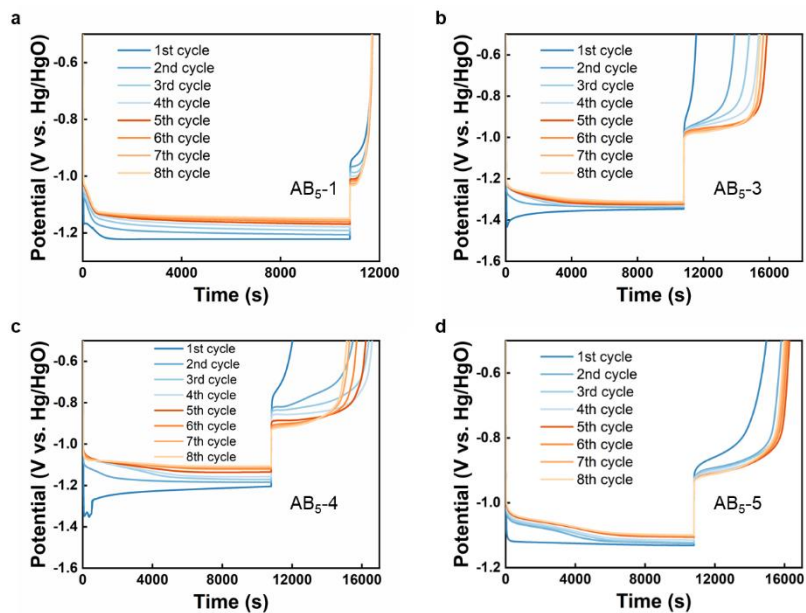
Fig.S3. Galvanostatic charge-discharge cycles for other four AB$_5$-type RR-electrodes studied in 6 M KOH solution. The RR-electrodes were charged at 30 mA for 3 h, and discharged at the same rate until electrode potential reached -0.5 V vs. Hg/HgO.
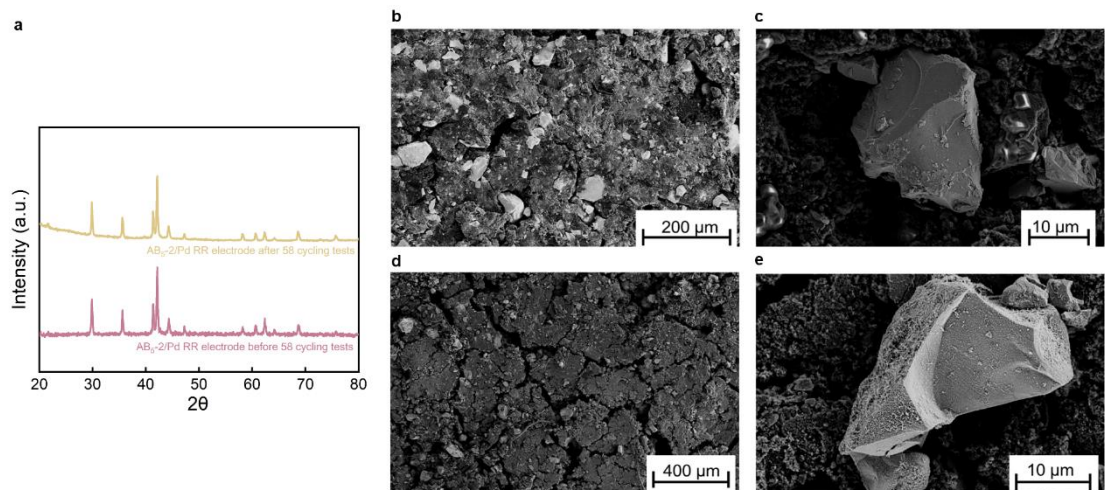
Fig.S4. The XRD patterns (a) and SEM images of the AB_5-2/Pd RR electrode before (b, c) and after 58 rounds of charge-discharge cycling tests (d, e).

a

Entry[a]	Temperature (°C)	Completion time (h)	Yield of Ethyl 3-phenylpropionate (%)
1	20	10	99
2[b]	20	10	97
3	35	5	95
4[b]	35	5	96
5	65	3	95
6[b]	65	3	97

b
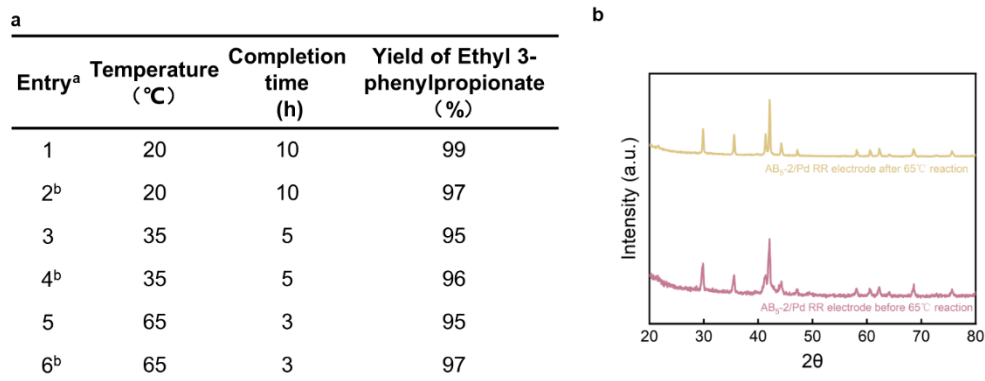
Fig.S5. Optimization of hydrogenation reaction temperature. a, Hydrogenation of ethyl cinnamate with charged AB_5-2/Pd electrode at different reaction temperature. [a]Ethyl cinnamate (0.067 M) in 15 mL THF solution was hydrogenated with the same alloy loading RR-electrodes at different temperature (20, 35, and 65 ℃), respectively. The reaction completion time of different reaction temperature was determined by sampling at hourly intervals. [b]Repeat experiments. **b**, XRD patterns of the AB_5-2/Pd electrode before and after 65℃ reaction.

Fig.S6. Galvanostatic charge-discharge cycles for AB$_5$-2 RR-electrode (a) and AB$_5$-2/Pd RR-electrode (b) studied in 6 M KOH solution. The RR-electrodes were charged at 30 mA for 3 h, and discharged at the same rat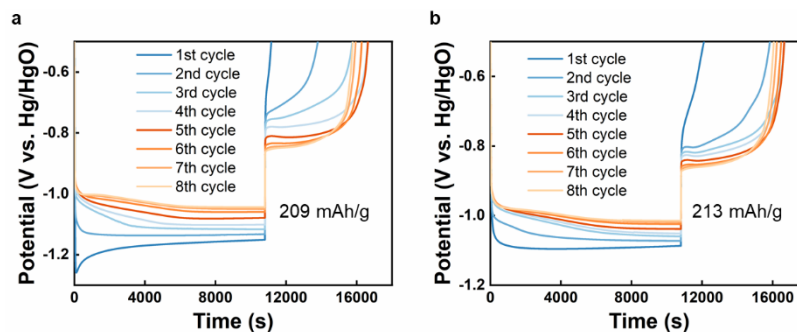e until electrode potential reached -0.5 V vs. Hg/HgO. The addition of Pd/C in the hydrogen storage material electrode did not cause noticeable differences in charging/discharging voltage and hydrogen storage capacity.

Table S2. Comparison of the catalytic hydrogenation activities of AB_5-2 RR-electrode and Pd/C.[a, b]

Entry	Catalyst	Yield of Ethyl 3-phenylpropionate (%)
1	Pd/C	95
2	AB_5-2 RR-electrode	3

[a]Reaction condition: 27 mg Pd/C (10 wt%) catalyst and the uncharged AB_5-2 RR-electrode were separately added into the sealed hydrogenation vessels containing 15 mL THF solution with 1.5 mmol ethyl cinnamate. The hydrogenation reactions were performed under room temperature with balloon H_2 for 10 h.

[b]The Pd/C catalyst exhibited high catalytic hydrogenation activity using the hydrogen gas cracked at catalyst surface as the hydrogen source, while the pristine AB_5-2 RR-electrode (with no H_{ads}) demonstrated almost no activity. And the catalytic performance is positively correlated with the H_{abs} concentration on AB_5 type alloy.[13] So, addition of the Pd/C catalyst in RR-electrode increased the catalytic activity under low H_{abs} concentration and successfully facilitated the usage of desorbed hydrogen gas.
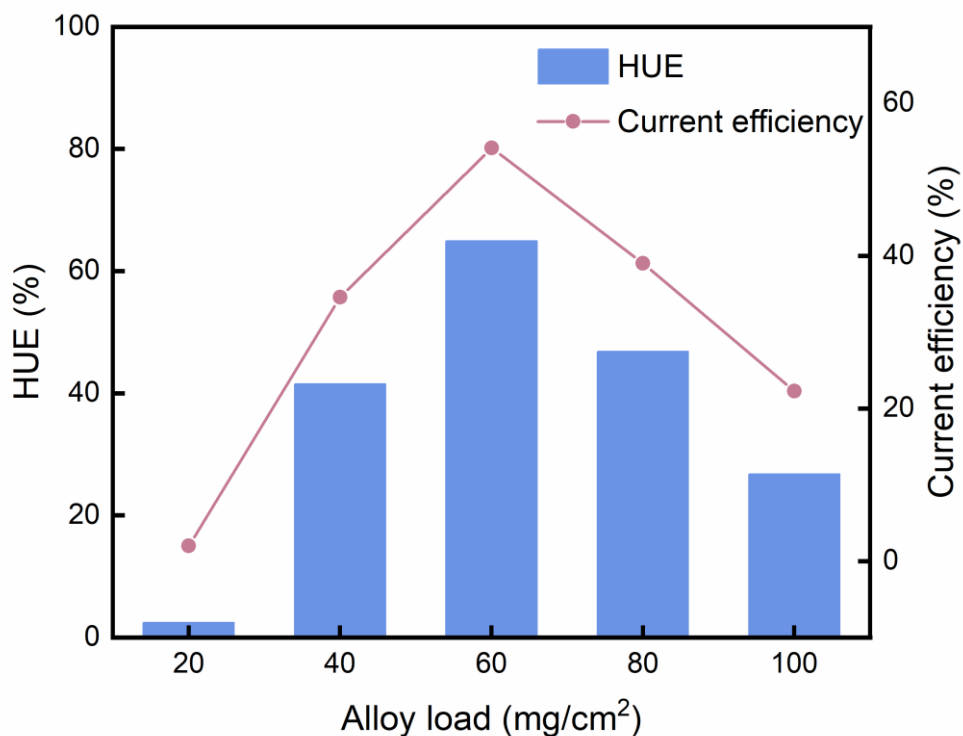
Fig.S7. The hydrogen utilization efficiency (HUE) and current efficiency of AB₅-2/Pd RR-electrodes with various alloy loadings. The HUE and current efficiency values of RR-electrodes (2 cm x 2 cm) were evaluated using the hydrogenation of 15 mL 0.067 M ethyl cinnamate THF solution. The current efficiencies were calculated based on the equation $(\frac{n_{utilized\ hydrogen\ atom} \times 96485}{Q_{passed\ charges}} \times 100\%)$. The electrons applied in the charging process were 1.2 equiv. of theoretical capacity of for RR-electrode.
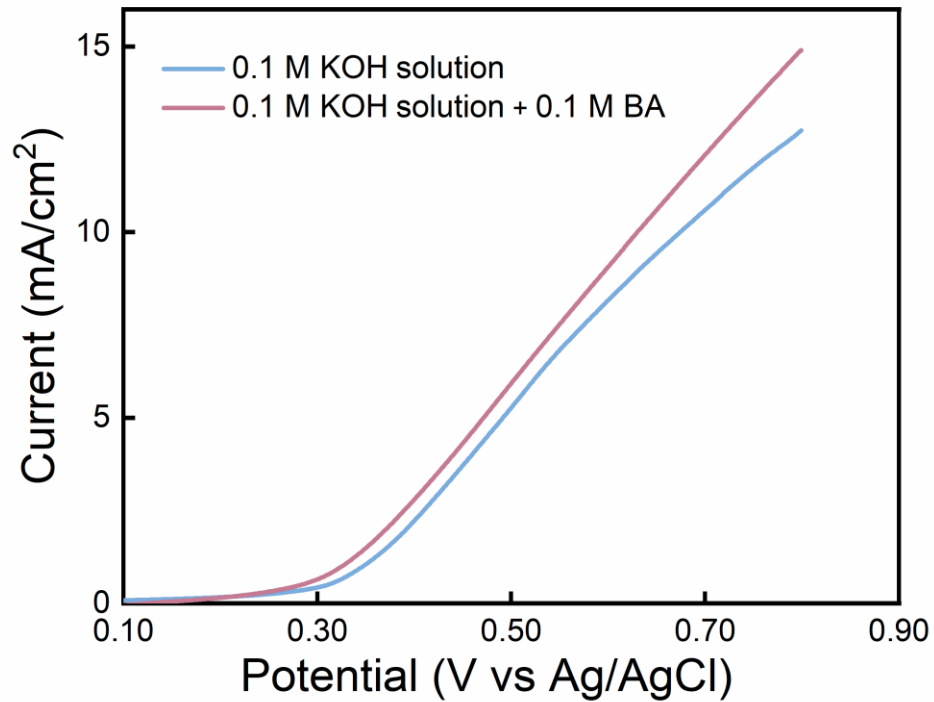
Fig.S8. Linear sweep voltammograms (LSV) of Ni(OH)$_2$/NF electrode. The testing condition: 0.1 M KOH aqueous solution with and without 0.1 M benzyl alcohol at a scan rate of 10 mV/s.

Table S3. Optimization of alcohol electrooxidation.[a]

Entry	Deviation	Electrooxidation	
		Yield of Benzaldehyde (%)	Yield of Benzoic acid (%)
1	-	5	93
2	NiOOH/NF (hydrothermal)[b]	8	80
3	Acetonitrile/water (1:1) solvent	11	74

[a]Reaction conditions: benzyl alcohol (0.025 M) dissolved in 0.1 M KOH t-BuOH/water solution (30 mL) was oxidized in an undivided cell under constant-current electrolysis (5 mA/cm^2) with (+) Ni(OH)$_2$/NF | (-) Pt. The yields of each product were determined by LC using mesitylene as an internal standard.

[b]The NiOOH/NF electrode applied in the entry 2 was prepared by hydrothermal method (Section 3.1).

Table S4. Comparison of RRP-eChem system with other different hydrogenation schemes.

Method	Membra-ne	Anodic reaction	Hydrogen source	Hydrogen utilization efficiency	Substrate scope	Electrolyte	Ref.
RRP-eChem	No	Alcohol oxidation	Water	59-70	C=C, C≡C, C=O, C=N, -CN, -NO$_2$	No	This work
Electrochemical hydrogation (ECH)	Yes/No	OER/amine oxidation	Water	78	C≡C	Yes	14
ECH	No	Ammonia oxdaition	Ammonia	-	C=C, C≡C, C=O	Yes	15
ECH	No	OER	Water	73	Nitrobenzene	Yes	16
Pd-membrane hydrogenation	Yes	Alcohol oxidation	Water	60-70	C=C, C≡C, C=O, C=N	No	17–20
Hydrogenation (in-situ usage of generated H$_2$)	Yes	OER	Water	60±18	Itaconic acid	Yes	21
Hydrogenation (ex-situ usage of generated H$_2$)	Yes/No	Alcohol oxidation and aldehyde oxidative condensation	Water/ MeOH	<40	C=C, hydrogenolysis	Yes	22
Thermal-hydrogenation[a]	No	-	Hydrogen	-	Unsaturated organic compound	Yes	23

[a]Require elevated temperature and pressure.

Table S5. Conventional paired electrolysis of benzyl alcohol oxidation and cathodic cinnamamide reduction.[a]

Entry	Anodic electrolyte	Cathodic electrolyte	Membrane	Yield of benzoic acid[b] (%)	Oxidation Selectivity (%)	Yield of 3-phenylpro panamide[b] (%)
1	0.05 M benzyl alcohol, 0.05 M cinnamamide, 0.1 M KOH in 4 mL DMSO/water (1:1)		-	10		-
2	0.05 M benzyl alcohol, 0.1 M KOH in 4 mL water	0.05 M cinnamami de, 0.1 M KOH in 4 mL MeOH	AEM[c] (AMI-7001S)	54.1	73	8
3			CEM[d] (Nafion 117)	10	21	47
4			CEM[e] (CMI-7000S)	18	33	27

[a]All the experiments were performed with a Ni(OH)$_2$/NF electrode (1 cm × 1 cm) as anode and a effectively electrohydrogenation catalyst[24] NiCoP/NF electrode (1 cm × 1 cm) as cathode at a 2 mA constant current for 15 h.

[b]The product yields were determined by LC using mesitylene as an internal standard.

[c]Anion exchange membrane (AMI-7001S, Membranes International, USA).

[d]Cation exchange membrane (Nafion 117, Duport).

[e]Cation exchange membrane (CMI-7000S, Membranes International, USA).

A

Entry	Membrane	MeOH in anodic cell (v%)[a]	Water in cathodic cell (v%)[a]
Entry 2 in Table S6	AEM (AMI-7001S)	7.43%	17.15%
Entry 3 in Table S6	CEM (Nafion 117)	3.59%	35.57%
Entry 4 in Table S6	CEM (CMI-7000S)	26.54%	7.52%

B
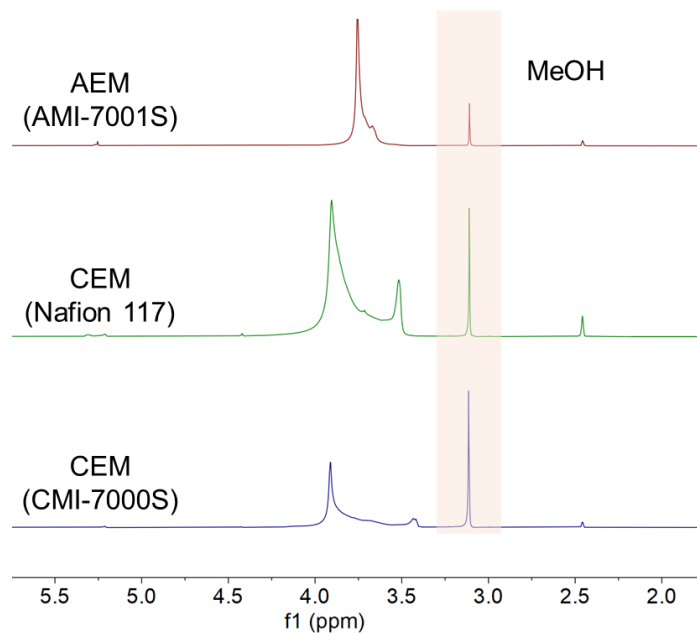
Fig.S9. The solvent cross-contamination determination of paired electrolysis of benzyl alcohol oxidation and cinnamamide reduction in the H-cell using ion exchange membranes. (A) The solvent cross-contamination determination. [a]The volumes of the crossover solvent were calculated from the ^{1}H NMR spectra using the dichloromethane as the internal standard. (B) ^{1}H NMR spectra of the solution in anodic compartments. MeOH solvent crossover was detected in all reactions (orange).

Table S6. Economic calculation of value of reductive transformation generated in the single-electrode electrolysis and RRP-eChem system for adipic acid production.

Parameters	Single-electrode electrolysis	RRP-eChem
Substrate	H_2O	p-Nitrotoluene
Substrate ($/ton)	-	1150[25]
Substrate ($/mol)	-	0.158
Product	H_2	p-Toluidine
Product ($/ton)	1400[21]	5000[26]
Product ($/mol)	0.0028	0.536
Production (ton/ton adipic acid)	0.087[a]	0.56[b]
122Value of reductive transformation ($/ton adipic acid)	122	1975

[a]The production of H_2 generated in the cathodic was calculated by the total pass charge in the single-electrode electrolysis of adipic acid in this work.

[b]The production of p-Toluidine generated in RRP-eChem system was calculated based on the scale-up experiment performed in this work.

[c]The value of reductive transformation was calculated based on the equation:

$$\frac{(Product\ (\$/mol) - Substrate\ (\$/mol))}{Mr_{product}\ (g/mol)} \times 10^6\ (g/ton) \times Production\ (ton/ton\ adipic\ acid).$$

Table S7. Images of RR-electrode immersed in several organic solvents and the discharge capacity of electrodes after long-term soaking.[a]

Images of RR-electrode in several organic solvent after 3 days	DCM	AC	CYH	ACN
Detachment	No	No	No	No
Discharge capacity (mAh)	188	205	199	201

[a]Reaction condition: The fully activated AB_5-2/Pd RR electrode with the same composition was immersed in different commonly used organic solvents, dichloromethane (DCM), acetone (AC), cyclohexane (CYH), and acetonitrile (ACN). The electrodes immersed in solvent were oscillated at a shaker for 3 days, then taken out to measure its discharge capacity. The RR-electrode was charged at 30 mA for 3 h, and discharged at the same rate until electrode potential reached -0.5 V vs. Hg/HgO.

2 Experiment Section

2.1 General information

All X-ray diffraction (XRD) measurements were carried out on an X-ray diffractometer (Bruker, D2 PHASER). The surface morphologies of alloy materials and RR-electrodes were examined using the scanning electron microscope (SEM) (Hitachi, SU8010, and Thermo Fisher Scientific, Scios 2 HiVac). The chemical compositions of the hydrogen storage alloys were determined using inductively coupled plasma-optical emission spectrometry (ICP-OES, Agilent 5800). The hydrogen pressure-composition isotherms of the alloy samples and RR-electrodes were measured using a high-pressure sorption analyzer (Beishide, BSD-PH). All electrochemical measurements, including cyclic voltammetry (CV) and linear sweep voltammetry (LSV), were conducted on a three-electrode setup with Hg/HgO or Ag/AgCl as the reference electrode at ambient conditions (BioLogic, SP-300). The reaction conversion and yield were determined by gas chromatography–mass spectrometry (GC–MS) (Agilent 8890–5977B) and liquid chromatography (LC) (Agilent 1260) using mesitylene as the internal standard.

2.2 Preparation of the redox-relay electrode and anode

Preparation of redox-relay electrode

The AB_5-type alloys studied in this work were obtained from Alfa Aesar (AB_5-1), Haoyun (AB_5-2 to AB_5-4), and Panasonic (AB_5-5). The commercial alloys powers were sieved to obtain particles with diameters within 20-100 μm range. The redox-relay electrodes were prepared using a slurry-coating method.[12] 90 wt% alloy powder, 5 wt% carbon black (ECP600JD), and 5 wt% PTFE solution (PolyFlon, D-210C) was mixed with 200 μL water in a mortar. 0.3 wt% Pd/C or Pt/C catalyst (based on Pd/Pt metal to the added AB_5 alloy) could be added to increase hydrogenation activity. The prepared alloy ink was then painted evenly on both sides of the carbon cloth (CeTech, W0S1011, 2 cm×2 cm). The painted electrodes were dried in vacuum at 200 ℃ for 2 h to remove the residual solvent. Before all tests, the prepared RR-electrodes were activated using an 8-cycle galvanostatic charge/discharge at a 0.33 C rate (equivalent to 124 mA/g based on the coated alloy amount) and discharge process stopped at a cut-off potential -0.5 V vs Hg/HgO. The relaxation time between each cycle is 30 minutes. The stability of the prepared RR-electrodes was examined in various organic solvents (Table S7).

Preparation of Ni(OH)$_2$/NF electrode

The nickel hydroxide anodes were prepared with an alternating-current electrophoretic deposition method (AC-EPD).[27] Before electrodeposition, the nickel foam (NF) was cleaned to remove surface oxides by sonication first in 3 M hydrochloric acid (HCl) solution for 6 min and then in DI water for 30 min. The electrodeposition aqueous solution was composed of 0.1 M nickel sulfate, 0.1 M sodium acetate, and 0.005 M sodium hydroxide. A 6.5 cm × 10 cm of the

cleaned NF electrode was immersed in the electrodeposition solution, and applied with a square-wave alternating current of ± 65 mA for 2000 cycles at ambient temperature (each cycle duration is 20 s). After AC-EPD, the electrodeposited NF electrode was rinsed with DI water, dried in air, and cut into 2 cm × 2 cm pieces for the electrooxidation of alcohols.

Preparation of NiOOH/NF electrode

The NiOOH/NF electrode was prepared with a hydrothermal method[28]. The nickel foam (NF) was cleaned firstly by sonicated in 3 M hydrochloric acid (HCl) solution for 6 min, and then in DI water for 30 min. The treated NF (2 cm × 2 cm) was placed in a 25 mL Teflon autoclave filled with a 15 mL aqueous solution containing 0.62 g of $NiCl_2 \cdot 6H_2O$ and 0.25 g of urea. The hydrothermal process was heated and kept at 100 °C for 12 h. The prepared electrode was cleaned with DI water, dried at 85 °C for 6 h, and finally annealed at 300 °C for 3 h under argon at an elevating temperature rate of 5 °C /min. The final NiOOH/NF electrode was conducted by 100 cycles of CV pretreatment in 1 M KOH solution at a scan rate of 50 mV/s to enrich the oxyhydroxide group (OOH^-).

Preparation of NiCoP/NF electrode

The NiCoP/NF electrode was prepared with a hydrothermal method[29]. The nickel foam (NF) was cleaned firstly by sonicated in 3 M hydrochloric acid (HCl) solution for 6 min, and then in DI water for 30 min. The treated NF (2 cm × 2 cm) was placed in a 25 mL Teflon autoclave filled with a 20 mL aqueous solution containing 0.291 g of $Co(NO_3)_2 \cdot 6H_2O$, 0.093 g of NH_4F and 0.25 g of urea. The hydrothermal process was heated and kept at 120 °C for 6 h. The prepared foam was cleaned with DI water and acetone, and dried under vacuum at 60 °C. The foam was loaded in a ceramic boat with 0.440 g of NaH_2PO_2 at the upstream side of the furnace. Then, the samples were heated at 300 °C for 1 h under argon.

2.3 Pressure-composition isotherms of alloys and corresponding electrode.

Three samples of AB_5 alloys (AB_5-1 and AB_5-2) and the corresponding AB_5-2 RR-electrode with a mass of 1.5 g were separately placed in a pressure reactor. The prepared AB_5-2 RR-electrode was cut into small pieces (0.1 × 0.1 cm) in order to fit into the reactor. Prior to the PCT measurements, all samples underwent four cycles of hydrogenation and dehydrogenation for activation. The activation cycling involved charging hydrogen at 40 bar and 343 K for 3 h, followed by discharging under vacuum at 423 K. The amount of absorbed hydrogen into the samples was calculated volumetrically. Pressure-composition isotherm measurements were carried out at 293 and 308 K using a BSD-PH apparatus. The pressure was varied from 0.1 to 4 bar with a step size of 0.05 bar for a duration of 0.5 h.

2.4 Characterization and procedure of the individual half-reactions

Hydrogenation of unsaturated substrates

All the prepared and activated RR-electrode (2 cm × 2 cm) was first fully charged in 0.1 M KOH solution at a constant current of 30 mA for 3 h with Ni(OH)$_2$/NF electrode (2 cm × 2 cm) as anode. Then, the charged RR-electrode was rinsed with DI water and transferred to a sealed hydrogenation vessel containing 15 mL THF solution with 1 mmol ethyl cinnamate, and then, kept at 35 °C in a shaker for 10 h.

The single-cycle pairing capacity per unit area (SCPC) and hydrogen utilization efficiency (HUE) are used as the evaluation criteria for hydrogen atom storage capacity and catalytic performance of the RR-electrode. SCPC and HUE are defined as follows:

$$SCPC = \frac{n_{utilized\ hydrogen\ atom}}{A_{RR-electrode}} = \frac{n_{hydrogenated\ product} \times n_e}{A_{RR-electrode}} \tag{1}$$

$$HUE = \frac{n_{utilized\ hydrogen\ atom}}{n_{maximum\ hydrogen\ atom\ storage\ capacity}} \times 100\% \tag{2}$$

$$Current\ efficiency = \frac{n_{utilized\ hydrogen\ atom} \times 96485}{Q_{passed\ charges}} \times 100\% \tag{3}$$

where $n_{utilized\ hydrogen}$ is the amount of the hydrogen atom utilized in the hydrogenation step, $n_{hydrogenated\ product}$ is the amount of the hydrogenated product, n_e is the theoretical number of electrons to produce 1 mol of the product, $A_{RR-electrode}$ is the area of RR-electrode, and $n_{maximum\ hydrogen\ atom\ storage\ capacity}$ is the maximum hydrogen atom storage capacity of AB$_5$ alloy calculated from PCT isotherm(a capacity of 1.24 wt% AB$_5$-2 alloy, which is equals to 12mmol H/g).

Electrocatalytic oxidation of alcohols

The electrolysis process was performed in an undivided cell with 30 mL 0.1 M KOH t-BuOH/water solution. The Ni(OH)$_2$/NF electrode (2 cm × 2 cm) and Pt mesh (1 cm × 1 cm) were used as the anode and cathode, respectively. The electrooxidation was conducted at a 30 mA constant current for 3 h. The experiment of replacing the Pt mesh cathode with RR-electrode was performed under the same condition. The yield and the FE of the products are calculated using the following equation:

$$Yield = \frac{n_{product}}{n_{substrate}} \times 100\% \tag{3}$$

$$FE = \frac{n_{product}}{Q/(F \times n_e)} \times 100\% \tag{4}$$

Where $n_{product}$ is the amount of the product, $n_{product}$ is the amount of the substrate, Q is the total charge passing through the electrode, F is the Faraday constant (96485 C/mol), and n_e is the theoretical number of electrons to produce 1 mol of the product R-COOH($n_e = 4$) and R_1COR_2 ($n_e = 2$).

2.5 Inductively coupled plasma-optical emission spectrometer (ICP-OES) study of AB$_5$-type hydrogen storge alloys and residual alloy after reaction.

Chemical composition measurement of the studied AB$_5$-type alloys

The precise chemical elemental compositions of the five LaNi$_5$-based materials were analyzed using inductively coupled plasma-optical emission spectroscopy (ICP-OES) employing the external standard method. All standard solution and samples were prepared using ultra-pure water. The bottles were soaked in an acid solution for one day and then rinsed with ultra-pure water. Multielement standard solutions (100 µg/mL, in 2.5 mol/L HCl, GSB 04-1767-2004; 100 µg/mL, in 1 mol/L HNO$_3$, GSB 04-1789-2004) were purchased from Guobiao (Beijing) Testing & Certification Co., Ltd. The calibration standard curves of several elements (Al, Ni, Co, Mn, La, Ce) were prepared ranged from to 4 ppm to 100 ppm through diluted by ultra-pure water. The following emission lines were used for quantification purposes: Al (308.215 nm and 396.152 nm), Ni (230.299 nm and 231.064 nm), Co (238.892 nm), Mn (257.61 nm), La (333.7 nm and 379.5 nm) and Ce (418.659 nm and 446.02 nm). Five alloy samples (0.1 g) were dissolved in the PTFE beakers using 10 mL of 1:1 HNO$_3$/water solution, respectively. After cooling, the digests were diluted to 100 mL with ultra-pure water Took out 5 ml of the diluted digestion solution and further diluted it by 10 times. Removal of insoluble impurities by filtration through a 45 µm filter prior to ICP analysis. Digestion blanks (in duplicate) were prepared using the same procedure as described above.

Measurement of leached alloy elements in the reaction crude of RRP-eChem system

The sample was prepared by removing 15 mL THF solvent of the hydrogenation reaction crude under vacuum, and adding 1 mL HNO$_3$/water (1:1) for dissolving potentially leached metallic elements. Subsequently, 14 mL of ultra-pure water was added to the flask. Removal of insoluble impurities by filtration through a 45 µm filter prior to ICP analysis. Two calibration standards curves of element La at 333.7 nm and 379.5 nm were prepared ranged from to 4 ppm to 100 ppm through diluted the multielement standard solution by ultra-pure water.
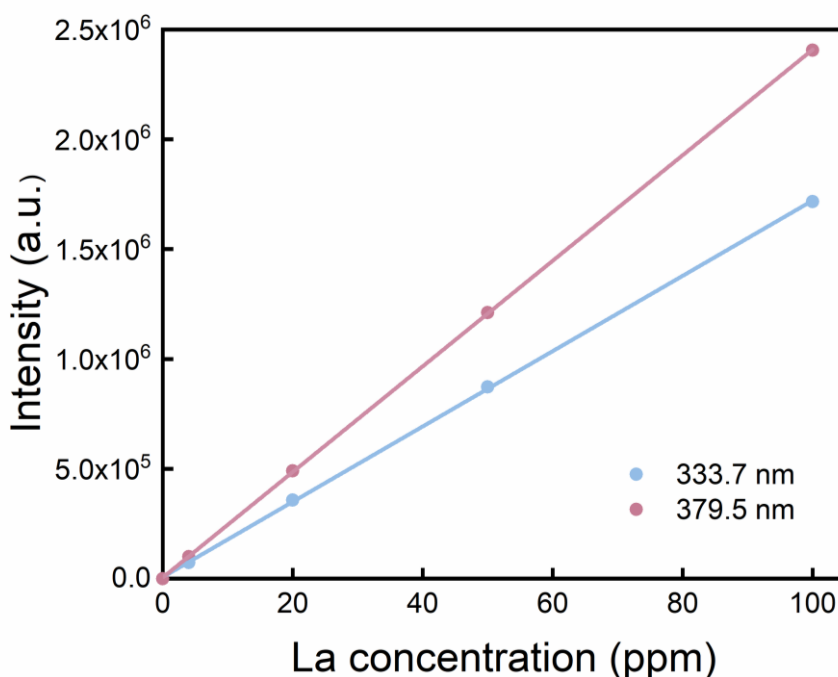
ICP-OES calibration curves of element La for 2 emission lines at 333.7 nm and 379.5 nm.

2.6 Procedure for redox-relay paired electrosynthesis

The RRP-eChem strategy is a two-step tandem electrochemical-chemical process. In the first electrochemical oxidation step, $Ni(OH)_2$/NF electrode (2 cm × 2 cm) and AB_5-2/Pd RR-electrode (2 cm × 2 cm with 60 mg/cm^2 alloy loading) functioned as anode and cathode, respectively. A 30 mL 0.1 M KOH t-BuOH/water solution containing 0.025 M primary alcohols and 0.05 M secondary alcohols substrate was electrolyzed at a 20 mA constant current for 6 h. After the completion of the electrolysis, the charged AB_5-2/Pd RR-electrode was rinsed with DI water, and transferred to the chemical hydrogenation vessel containing unsaturated substrate (C=C (0.053 M), C≡C (0.027 M), C=O (0.053 M), C=N (0.053 M), -CN (0.027 M), and -NO_2 (0.017 M) unsaturated groups) in 15 mL THF or MeOH. The hydrogenation step was performed at 35 °C for 5 h. The RR-electrode can be reused for the next round of RRP-eChem after rinsing.

2.7 Scaled-up RRP-eChem synthesis of adipic acid and p-toluidine

An AB_5-2/Pd RR-electrode (27 cm × 8 cm with 13 g AB_5-2 alloy loading) and a $Ni(OH)_2$-SDS/NF anode (16 cm × 8 cm) was positioned on the electrode holder (Supplementary Information Section 4). In the first electrooxidation step, an 800 mL 1 M KOH solution containing 0.5 M cyclohexanone was electrolyzed at 800 mA current for 6 h. Subsequently, the electrode holder containing the charged AB_5-2/Pd RR-electrode was rinsed with DI water, and transferred to the chemical hydrogenation vessel containing 800 mL 0.019 M p-nitrotoluene MeOH solution.

The hydrogenation process was carried out at room temperature for 10 h. The single-electrode ADP electrosynthesis was performed using the same reaction conditions with NF electrode (27 cm × 8 cm) as the cathode.

2.8 Operation of the automated RRP-eChem platform

The automated RRP-eChem platform consists of three main components, including an electrode holder attached on an X-Z axis cartesian robot, a reagent solution pumping module, and three cells for reaction and rinsing. An AB_5-2/Pd RR-electrode (2.5 cm × 11 cm with 1.65 g AB_5-2 alloy loading), a $Ni(OH)_2$/NF electrode (2 pieces of 2 cm × 3 cm), a Pt wire (1 mm diameter), and an Ag/AgCl reference electrode was installed on the electrode holder. The reagent solution pumping module included a peristaltic pump and two 8-port selection valves to inject and withdraw reagent solutions into and out of each cell, respectively. The whole platform was controlled using a customized LabVIEW program. Detailed descriptions of the hardware and software can be found in supplementary information.

The automated four-step procedure for redox-relay paired electrosynthesis is described as follows: (1) Electrode activation: 50 mL 6 M KOH activation solution was transferred into cell A for activating AB_5-2/Pd RR-electrode. The AB_5-2/Pd RR-electrode was activated with a 4-cycle galvanostatic charge/discharge process at 0.17 C rate with Pt wire as the counter electrode, with a cut-off discharge potential -0.6 V vs Ag/AgCl. After electrode activation, DI water and methanol were used for rinsing cell A and electrodes, respectively. (2) Electrooxidation: 60 mL 0.1 M KOH t-BuOH/water solution containing 0.05 M benzyl alcohol was fed into Cell A. The $Ni(OH)_2$/NF electrode and AB_5-2/Pd RR-electrode were used as the anode and cathode, respectively. The electrooxidation process was performed under 50 mA constant current at ambient temperature for 13 h. (3) Electrode rinsing: Following the electrooxidation process, the electrodes were taken out from Cell A, and rinsed in Cell B using 40 mL DI water. (4) Hydrogenation: The electrode holder was moved to Cell C which was pre-filled with 50 mL 0.12 M cinnamamide methanol solution. The hydrogenation process was carried out at 35 ℃ for 10 h. The electrodes on the electrode holder were reused for the next round of the RRP-eChem cycle, and the $Ni(OH)_2$/NF electrode was replaced with a new piece after each five cycles to achieve consistent performance for alcohol electrooxidation.

3 Detailed design of the electrode assembly for scaled-up RRP-eChem

3.1 Preparation of Ni(OH)$_2$-SDS/NF electrode

The Ni(OH)$_2$-SDS/NF electrode was prepared with a hydrothermal method[30]. The nickel foam (NF) was cleaned firstly by sonicated in 0.5 M hydrochloric acid (HCl) solution for 15 min, and then in ethanol, DI water for 15 min, separately. The treated NF (8 cm × 16 cm) was placed in a 1 L Teflon autoclave filled with a 700 mL well-mixed aqueous solution containing Ni(NO$_3$)$_2$·6H$_2$O (26.25 mmol), NH$_4$F (72.8 mmol), urea (290.5 mmol) and SDS (52.5 mmol). The hydrothermal process was heated and kept at 100 °C for 10 h. The prepared electrode was cleaned with DI water, dried at 60 °C for 12 h.

3.2 Detailed dual-loop electrode assembly

For the scaled-up RRP-eChem system, we engineered a loop electrode holder for placing the larger RR-electrode area in limited electrolyte volume. An AB$_5$-2/Pd RR-electrode (27 cm × 8 cm with 13 g AB$_5$-2 alloy loading) and a Ni(OH)$_2$-SDS/NF anode (16 cm × 8 cm) was positioned on the outer and inner rings of the electrode holder, separately. Nickel film (8) was used as the cathode current collector.
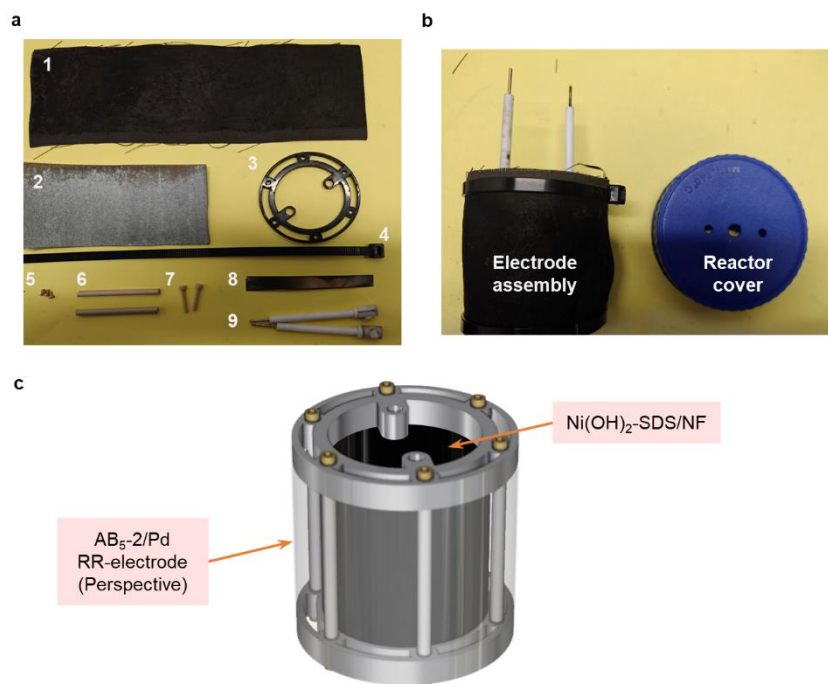
**The photos of electrode components (a), electrode assembly (b), and the schematic (c) of dual-loop electrode assembly.** (1: 27 cm × 8 cm AB$_5$-2/Pd RR-electrode, 2: 16 cm × 8 cm Ni(OH)$_2$-SDS/NF anode, 3: PP shell, 4: PP cable ties, 5: Φ2 mm Peek screws, 6: Φ4 mm Peek rod × 70 mm, 7: Φ3 mm Peek screws, 8: Nickel film current collection, 9: Pt electrode clamps)

4 Detailed design of the automated RRP-eChem platform.

4.1 Hardware setup

This automated platform consists of a four-electrode assembly attached on an X-Z axis cartesian robot system as the end effector connected to an electrochemical workstations (SP-300), a set of eChem reactors containing: 1) an electrochemical oxidation cell A, 2) an electrode rinsing cell B and 3) a hydrogenation cell C, two 8-port selection valves, a peristaltic pump, and a reactant supply and production crude collection module, as shown in the figure below.
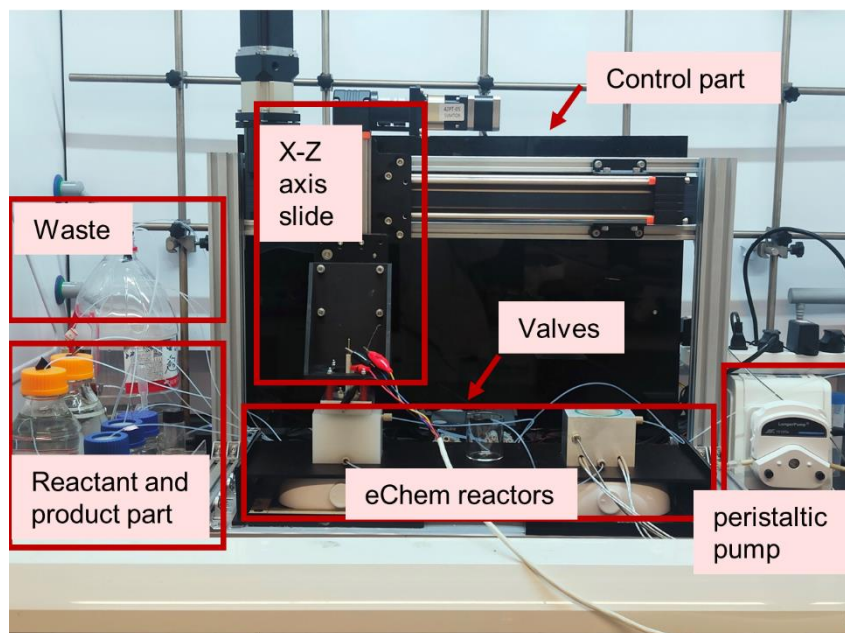
The image of the automated RRP-eChem platform

4.2 Solution delivery

All the liquids (reaction solution, rinse solution, product, waste) applied in the RRP-eChem platform are delivered through different tubing connected with selection valves. Waste liquid and air channels were connected using 1/8" OD PFA tubing. Other liquid tubes were 1/16'' OD PFA tubes. Two valves are connected in series by linking their central positions. Valve 1 was connected to the reactant supply and production crude collection containers, while Valve 2 was connected to the eChem reactors. By switching the position of the valves and changing the direction of the peristaltic pump through LabVIEW program, functions such as solvent feeding, product collection, and reactor and pipeline cleaning can be achieved. The detailed interconnections between all liquid containers and the e-Chem reactors in the RRP-eChem system are presented in the following schematic and list:
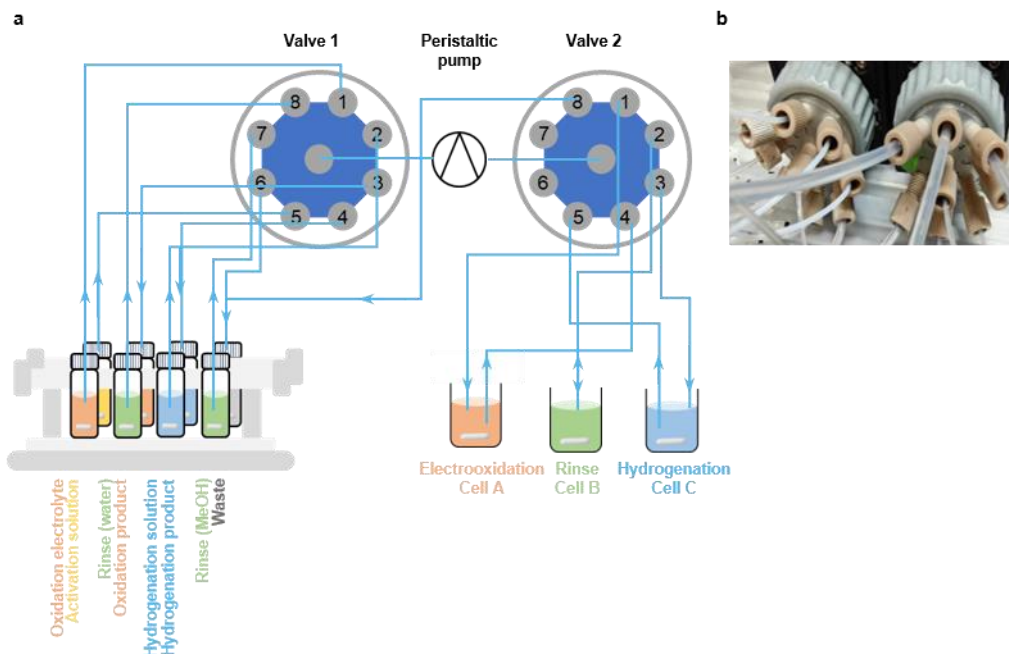
The schematic (a) and photo (b) of solution pumping module

Detailed interconnections of valves

Liquid containers/ Reactors	Position
Alcohol oxidation electrolyte (S1)	V1-1
Hydrogenation solution (S2)	V1-2
Electrochemical product (P1)	V1-3
Hydrogenation product (P2)	V1-4
Activation solution	V1-5
Waste	V1-6
Methanol (Rinse)	V1-7
Water (Rinse)	V1-8
Electrolysis cell A (inlet)	V2-1
Wash bottle B	V2-2
Hydrogenation reactor C (inlet)	V2-3
Electrolysis cell A (outlet)	V2-4
Hydrogenation reactor C (outlet)	V2-5
Air	V2-6
Waste	V2-8

4.3 Detailed four-electrode assembly

A four-electrode cell configuration (see the below figure) for this platform was assembled as the end effector on the cartesian robot, composed of an ring-type AB_5-2/Pd RR-electrode (2.5 cm × 11 cm, with 1.65 g alloy loading), a $Ni(OH)_2$/NF electrode (2 cm × 3 cm, 2 pieces), a Pt wire

(1 mm diameter) and an Ag/AgCl reference electrode. For the activation process, the RR-electrode was connected as the working electrode with a Pt wire as the counter electrode and an Ag/AgCl electrode as the reference electrode. The electrochemical oxidation was conducted with a typical two-electrode system, which used a $Ni(OH)_2$/NF electrode and the RR-electrode as the anode and cathode, respectively. As for the hydrogenation process, the connection between the electrodes and the electrochemical workstation would be temporarily disconnected. The switching and disconnection of the operating circuit was achieved through relay controlled by the preprogrammed procedure using LabVIEW 2020.
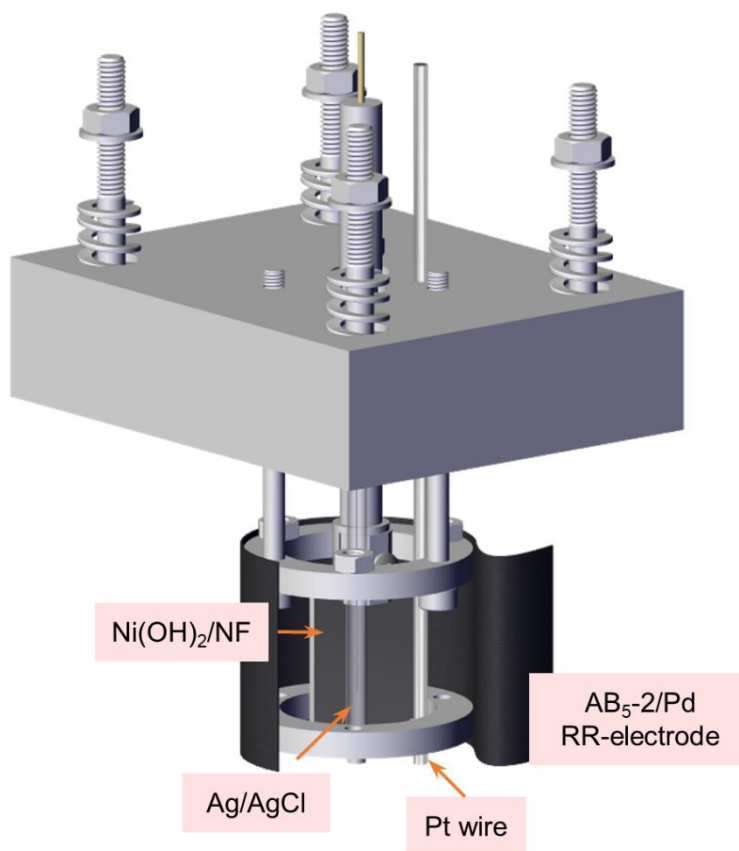
The schematic of the Four-electrode cell configuration

4.4 eChem reactors:

The eChem reactors, shown in the figure below, consist of a PP electrooxidation cell (A), an electrode rinsing cell (B) (not shown), and a hydrogenation cell (C). To meet the different optimal temperature requirements in the second hydrogenation step, the cylindrical PP reactor B is enclosed in an aluminum shell with high thermal conductivity. This shell is embedded with two heating rods connected to a heating device and a thermocouple wire for temperature

measurement. Mixing in the reactors is achieved using inner magnetic stir bars controlled by a magnetic stirrer located behind the reactors.
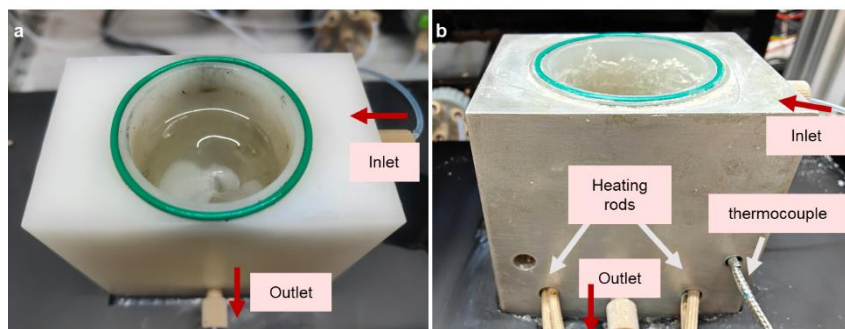
The image of the electrooxidation cell A (a) and hydrogenation cell C (b)

4.5 System control software

The step-by step procedures of electrode activation, electrooxidation, electrode rinsing and hydrogenation are controlled by custom LabVIEW 2020 codes, as well as the hardware communications. The code is structured for usability and can be easily modified to meet specific application requirements. System parameters such as reagent volume, reaction temperature, and reaction time are pre-defined in the LabVIEW user interface. The front-end graphical display enables users to monitor the automation platform's status, both on-site and remotely, as shown in the figure below. The detailed steps of the custom LabVIEW code procedure were provided in the following table. The valve switching steps are not included in the table, as they are described in detail in section 5.1.1.
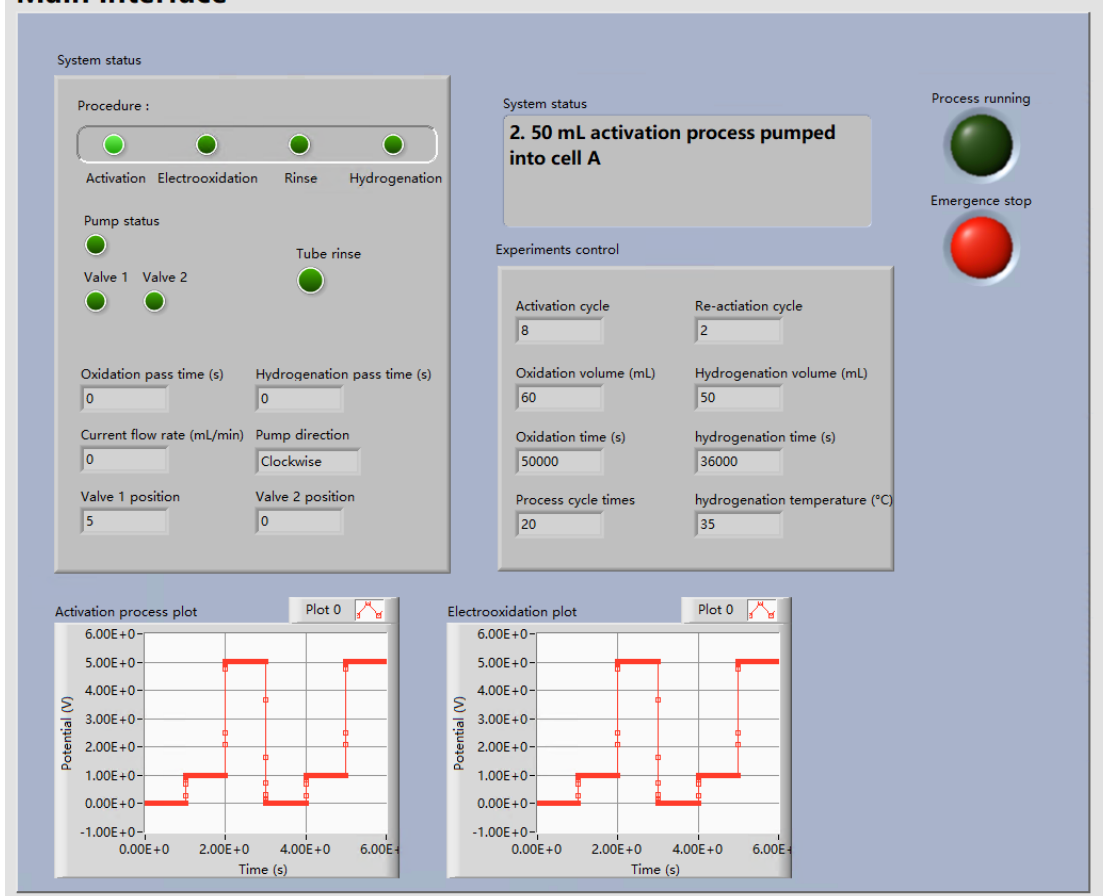
LabVIEW front-end interface for the automated RRP-eChem platform

Detail step of LabVIEW code

Procedure		Instrument	Step
1 Electrode activation	1.1	Pump	Rinse the channel with activation solution
	1.2	Pump	Load 50 mL activation solution into Cell A
	1.3	Robot	Load the x-axis position to "50 mm", Load the z-axis position to "150 mm"
	1.4	Potentiostat	Conduct galvanostatic charge/discharge process
	1.5	Pump	Pump the activation solution back to storage containers
	1.6	Pump	Load 50 mL DI water into Cell A
	1.7	Robot	Load the z-axis position to "80 mm", and then to "150 mm", alternatively 3 times for electrode rinse, then to "0 mm"
	1.8	Pump	Pump the water to waste containers
	1.9	Pump	Load the rinse methanol into Cell A
	1.10		Stir for 1 min

	1.11	Pump	Pump the rinse methanol to waste containers
2 Electrooxidation	2.1	Pump	Rinse the channel with electrooxidation solution
	2.2	Pump	Load 60 mL activation solution into Cell A
	2.3	Robot	Load the z-axis position to "150 mm"
	2.4	Potentiostat	Conduct electrooxidation process for 46800 s
3 Electrode rinse	3.1	Pump	Load 40 mL DI water into Cell B
4 Hydrogenation	4.1	Pump	Rinse the channel with hydrogenation solution
	4.2	Pump	Load 50 mL hydrogenation solution into Cell C
3 Electrode rinse	3.2	Robot	Load the z-axis position to "0 mm", Load the x-axis position to "1500 mm".
	3.3	Robot	Load the z-axis position to "150 mm", and then to "80 mm", alternatively 3 times for electrode rinse, then to "0 mm"
4 Hydrogenation	4.3	Robot	Load the x-axis position to "3140 mm", Load the Z-axis position to "150 mm".
		Heat module	Heat hydrogenation solution to 35 °C, keep for 36000
2 Electrooxidation	2.5	Pump	Collect electrooxidation product to storage container
	2.6	Pump	Load 50 mL DI water into Cell A
	2.7	Pump	Pump the water to waste containers
	2.8	Pump	Load the rinse methanol into Cell A
	2.9		Stir for 1 min
	2.10	Pump	Pump the rinse methanol to waste containers
3 Electrode rinse	3.4	Pump	Pump the water on the Cell B to waste containers
4 Hydrogenation	4.4	Pump	Rinse the channel with water
	4.5	Robot	Load the Z-axis position to "0 mm".
	4.6	Pump	Collect hydrogenation product to storage container
	4.7	Pump	Load 50 mL DI water into Cell C
	4.8	Robot	Load the z-axis position to "150 mm", and then to "80 mm", alternatively 3 times for electrode rinse, then to "0 mm"
	4.9	Pump	Pump the water to waste containers
	4.10	Pump	Load the rinse methanol into Cell C
	4.11		Stir for 1 min
	4.12	Pump	Pump the rinse methanol to waste containers

5 References:

1   Y. Sekine and T. Higo, *Top. Catal.*, 2021, 64, 470–480.

2   F. Wang, W. Li, R. Wang, T. Guo, H. Sheng, H.-C. Fu, S. S. Stahl and S. Jin, *Joule*, 2021, 5, 149–165.

3   K. H. Michael, Z.-M. Su, R. Wang, H. Sheng, W. Li, F. Wang, S. S. Stahl and S. Jin, *J. Am. Chem. Soc.*, 2022, 144, 22641–22650.

4   R. Wang, H. Sheng, F. Wang, W. Li, D. S. Roberts and S. Jin, *ACS Cent. Sci.*, 2021, 7, 2083–2091.

5   Y. Gu, J. Wei, X. Wu and X. Liu, *Sci. Rep.*, 2021, 11, 11136.

6   D. Bresser, D. Buchholz, A. Moretti, A. Varzi and S. Passerini, *Energy Environ. Sci.*, 2018, 11, 3096–3127.

7   D. Li and M. Liao, *J. Fluor. Chem.*, 2017, 201, 55–67.

8   State Key Lab of Oil and Gas Reservoir Geology & Exploitation, Southwest Petroleum University, Chengdu 610500, China and Z. Zhu, *Int. J. Electrochem. Sci.*, 2016, 8270–8279.

9   S. Liu, K. Wippermann and W. Lehnert, *Int. J. Hydrog. Energy*, 2021, 46, 14687–14698.

10 R. Friedmann and T. Van Nguyen, *J. Electrochem. Soc.*, 2010, 157, B260.

11 F. Mack, T. Morawietz, R. Hiesgen, D. Kramer, V. Gogel and R. Zeis, *Int. J. Hydrog. Energy*, 2016, 41, 7475–7483.

12 C. Khaldi, H. Mathlouthi and J. Lamloumi, *J. Alloys Compd.*, 2009, 469, 464–471.

13 R. Tsukuda, T. Kojima, Y. Xu, C. Nishimura, M. Krajčí and S. Kameoka, *J. Phys. Chem. C*, 2021, 125, 20919–20929.

14 Y. Wu, C. Liu, C. Wang, S. Lu and B. Zhang, *Angew. Chem. Int. Ed.*, 2020, 59, 21170–21175.

15 J. Li, L. He, X. Liu, X. Cheng and G. Li, *Angew. Chem. Int. Ed.*, 2019, 58, 1759–1763.

16 D. Carvajal, R. Arcas, C. A. Mesa, S. Giménez, F. Fabregat-Santiago and E. Mas-Marzá, *Adv. Sustain. Syst.*, 2022, 6, 2100367.

17 R. S. Sherbo, R. S. Delima, V. A. Chiykowski, B. P. MacLeod and C. P. Berlinguette, *Nat. Catal.*, 2018, 1, 501–507.

18 R. S. Sherbo, A. Kurimoto, C. M. Brown and C. P. Berlinguette, *J. Am. Chem. Soc.*, 2019, 141, 7815–7821.

19 R. S. Delima, M. D. Stankovic, B. P. MacLeod, A. G. Fink, M. B. Rooney, A. Huang, R. P. Jansonius, D. J. Dvorak and C. P. Berlinguette, *Energy Environ. Sci.*, 2022, 15, 215–224.

20 Y.-Q. Yan, Y. Chen, Z. Wang, L.-H. Chen, H.-L. Tang and B.-L. Su, *Nat. Commun.*, 2023, 14, 2106.

21 K. Obata, M. Schwarze, T. A. Thiel, X. Zhang, B. Radhakrishnan, I. Y. Ahmet, R. Van De Krol, R. Schomäcker and F. F. Abdi, *Nat. Commun.*, 2023, 14, 6017.

22 T. Wu, B. H. Nguyen, M. C. Daugherty and K. D. Moeller, *Angew. Chem. Int. Ed.*, 2019, 58, 3562–3565.

23 A. W. Langer, J. Stewart, C. E. Thompson, H. T. White and R. M. Hill, *Ind. Eng. Chem.*, 1961, 53, 27–30.

24 T. Mou, J. Liang, Z. Ma, L. Zhang, Y. Lin, T. Li, Q. Liu, Y. Luo, Y. Liu, S. Gao, H. Zhao, A. M. Asiri, D. Ma and X. Sun, *J. Mater. Chem. A*, 2021, 9, 24268–24275.

25 Stabilization of Asian Nitrotoluene Prices in August 2023: Implications for Upstream and Downstream Value Chains, https://www.chemanalyst.com/NewsAndDeals/NewsDetails/stabilization-of-asian-nitrotoluene-prices-in-august-2023-implications-for-upstream-19153, (accessed December 7, 2023).

26 [Hot Item] Factory CAS 106-49-0 P-Toluidine for Dye Intermediate, https://guanlangbio.en.made-in-china.com/product/PFraWtcAsTYj/China-Factory-CAS-106-49-0-P-Toluidine-for-Dye-Intermediate.html, (accessed December 7, 2023).

27 *Tetrahedron*, 1982, 38, 3299–3308.

28 T. Eisa, H. O. Mohamed, Y.-J. Choi, S.-G. Park, R. Ali, M. A. Abdelkareem, S.-E. Oh and K.-J. Chae, *Int. J. Hydrog. Energy*, 2020, 45, 5948–5959.

29 W. Li, X. Gao, X. Wang, D. Xiong, P.-P. Huang, W.-G. Song, X. Bao and L. Liu, *J. Power Sources*, 2016, 330, 156–166.

30 Z. Li, X. Li, H. Zhou, Y. Xu, S.-M. Xu, Y. Ren, Y. Yan, J. Yang, K. Ji, L. Li, M. Xu, M. Shao, X. Kong, X. Sun and H. Duan, *Nat. Commun.*, 2022, 13, 5009.